A round-robin study on the tensile characterization of single fibres: A multifactorial analysis and recommendations for more reliable results

Thomas Jeannin, Gilles Arnold, Alain Bourmaud, Stéphane Corn, Emmanuel de Luycker, Pierre J.J. Dumont, Manuela Ferreira, Camille François, Marie Grégoire, Omar Harzallah, et al.

Journal Pre-proofs

A round-robin study on the tensile characterization of single fibres: A multi-factorial analysis and recommendations for more reliable results

Thomas Jeannin, Gilles Arnold, Alain Bourmaud, Stéphane Corn, Emmanuel De Luycker, Pierre J.J. Dumont, Manuela Ferreira, Camille François, Marie Grégoire, Omar Harzallah, Julie Heurtel, Sébastien Joannès, Antoine Kervoelen, Ahmad Rashed Labanieh, Nicolas Le Moigne, Florian Martoïa, Laurent Orgéas, Pierre Ouagne, Damien Soulat, Alexandre Vivet, Vincent Placet

PII: S1359-835X(24)00320-8
DOI: https://doi.org/10.1016/j.compositesa.2024.108323
Reference: JCOMA 108323

To appear in: *Composites: Part A*

Received Date: 5 April 2024
Revised Date: 14 June 2024
Accepted Date: 16 June 2024

Please cite this article as: Jeannin, T., Arnold, G., Bourmaud, A., Corn, S., De Luycker, E., Dumont, P.J.J., Ferreira, M., François, C., Grégoire, M., Harzallah, O., Heurtel, J., Joannès, S., Kervoelen, A., Rashed Labanieh, A., Le Moigne, N., Martoïa, F., Orgéas, L., Ouagne, P., Soulat, D., Vivet, A., Placet, V., A round-robin study on the tensile characterization of single fibres: A multifactorial analysis and recommendations for more reliable results, *Composites: Part A* (2024), doi: https://doi.org/10.1016/j.compositesa.2024.108323

A round-robin study on the tensile characterization of single fibres: a multifactorial analysis and recommendations for more reliable results

Thomas Jeannin[a], Gilles Arnold[b], Alain Bourmaud[c], Stéphane Corn[d], Emmanuel De Luycker[e], Pierre J.J. Dumont[f], Manuela Ferreira[g], Camille François[b], Marie Grégoire[e], Omar Harzallah[b], Julie Heurtel[h], Sébastien Joannès[h], Antoine Kervoelen[c], Ahmad Rashed Labanieh[g], Nicolas Le Moigne[i], Florian Martoïa[f], Laurent Orgéas[j], Pierre Ouagne[e], Damien Soulat[g], Alexandre Vivet[k], Vincent Placet[a]

[a] Université de Franche-Comté, CNRS, institut FEMTO-ST, 25000, Besançon, France

[b] Université de Haute-Alsace, LPMT UR 4365, 68093 Mulhouse, France

[c] Univ. Bretagne Sud, UMR CNRS 6027, IRDL, F-56100 Lorient, France

[d] LMGC, IMT Mines Alès, Univ Montpellier, CNRS, Alès, France

[e] Univ. de Toulouse, Laboratoire Génie de Production, LGP, INP-ENIT, F-65016 Tarbes, France

[f] Univ. Lyon, INSA Lyon, CNRS, LaMCoS, UMR5259, 69621 Villeurbanne, France

[g] Univ. Lille, ENSAIT, GEMTEX – Laboratoire de Génie et Matériaux Textiles, 59056, Roubaix, France

[h] Mines Paris, Université PSL, Centre des Matériaux (MAT), UMR 7633 CNRS, 91003 Evry, France

[i] Polymers Composites and Hybrids (PCH), IMT Mines Alès, Alès, France

[j] University of Grenoble Alpes, CNRS, Grenoble INP, 3SR Lab, F-38000 Grenoble, France

[k] Normandie Univ, ENSICAEN, UNICAEN, CEA, CNRS, CIMAP, 14000 Caen, France

Abstract

In this benchmark, the tensile properties of three types of organic fibres – flax, hemp and aramid - were determined using single-fibre tensile tests performed by nine research groups. Flax and hemp were chosen due to their prevalence among European fibre plants. Aramid was selected for its synthetic nature and comparable dimensional properties. Due to the morphological complexity and variability of plant fibres, the scatter in the apparent tangent modulus and strength is more pronounced for flax and hemp compared to aramid. The primary source of scatter in the tensile properties results from human factors and experimental procedures, particularly regarding the fibre selection, the measurement of the fibre cross-sectional area and of the tensile strain. The post-processing procedure also turns out to be a key factor. Finally, recommendations and guidelines for best practices are proposed to reduce the main sources of dispersion associated with the reproducibility of single fibre tensile tests.

Keywords: A. Aramid fibres, A. Natural fibres, B. Mechanical properties, D. Mechanical testing

1. Introduction

Over the past 20 years, the determination of the mechanical properties of fibres, especially in tension, has been the subject of a very large number of studies, for various applications and types of fibres. As detailed, for example in references [1–3] for plant fibres, 3 types of tests are commonly used: tensile tests on single fibre (i.e., individual elementary fibre), tensile tests on bundle of fibres (i.e., group of elementary fibres), and the inverse method IFBT (Impregnated Fibre Bundle Testing [4–7]). Besides, the resurgence in fibre characterization studies is primarily linked to several major industrial facts. First, the biocomposite market (which includes wood fibre composites and plant fibre composites) is expected to grow from 24.40 billion USD achieved in 2021 to 90.89 billion USD in 2030 [8], which requires an in-depth understanding of the properties of plant fibres, most commonly used in these biocomposites, for a very wide range of fibre sources [9–13]. Second, there is a growing interest in the

reuse of fibres either from production waste [14,15] or recycled from composite waste [16–20]. Also, regarding virgin synthetic fibres, tensile tests on elementary fibres are used to investigate the impact of sizing [21], to compare tensile behaviour of carbon/glass fibres [22] or to optimize various types of PAN (PolyAcryloNitrile)-based carbon fibres, which tensile behaviour shows non-linear responses [23].

All these studies have in common that they pertain to fibres of various finite lengths (for both plant fibres and recycled synthetic fibres), which induce limitations in conducting: (i) tensile tests on bundle and particularly to guarantee that all the fibres in these bundles are gripped between the machine jaws; (ii) the IFBT method and bundle testing to guarantee a controlled orientation of the fibres in the direction of the applied force. As a result, most studies focus on the use of tensile tests on elementary fibres. This method is complex and time-consuming due to the small dimensions of the fibres that have to be individualized, which can also be a source of damage [24]. Several standards, including ASTM C1557 [25], ASTM D3822 [26] and NF T25-501-2 [27], have been specifically developed for conducting tensile tests on single fibres. ASTM C1557 focuses on determining the tensile strength and Young's modulus of advanced ceramic, glass, carbon and other fibres. ASTM D3822 is designed for assessing the tensile properties of both natural and synthetic fibres. Additionally, NFT25-501-2 is intended for the determination of the tensile properties of single flax fibres. These standards offer guidelines for conducting tensile testing procedures.

Using tensile tests, many authors have analysed the phenomena and parameters that could lead to significant inaccuracies and large scattering in the measurement of mechanical properties [1,2,28–31]. In the case of synthetic fibres such as glass, carbon and aramid, having regular cross-sectional shape, the sampling procedure greatly influences the uncertainty in the tensile properties [32,33]. For plant fibres such as hemp and flax, which have non-regular cross-sectional shapes, results show (e.g. flax, [34]) that while the uncertainty in the elongation is minimal, the total uncertainty, integrating all experimental factors, can be as high as 25% and 49% of the standard deviation of the experimentally determined stress at break and the elastic modulus, respectively. The cross-sectional area (CSA) measurement method is a crucial factor to determine the tensile properties (tangent modulus, strength) of elementary fibres, and several approaches have been reported in the literature. For many years, the major method used to estimate the CSA is based on the estimation of the average apparent fibre diameter from optical microscopy, which is equivalent to consider fibres as perfect cylinders. This is a very biased hypothesis [35] given the wide diversity of full or hollow cross-sectional shapes encountered with plant fibres [36] as well as elliptical cross-sections found in synthetic ones too [37]. Besides, flax fibre's cross-sections were shown to significantly vary along their length, the coefficient of variation in diameter reaching about 20% for e.g. flax fibres [28,36,38,39]. If one views the fibre as a chain of elements with varying sections, a model proposed in [49] suggests that the fibre's elastic modulus can increase by 12% compared to a value calculated on an average elliptical cross-section [39]. This is even more critical for tensile strength where differences up to 200% can arise between the strength calculated using the minimal cross section (possibly the weakest point of the fibre) and that calculated using the average cross section [40,49]. Using optical microscopy, high resolution flat-bed scanning and automated laser scanning for fibre dimensional analysis, Haag and Mussig [30] demonstrated up to 300% variation in tensile strength values according to the calculated CSA. The contrasted morphometric characteristics of plant fibres and their specific cross-sectional shape must also be considered with adapted geometrical models (e.g. circular, elliptic …) for the calculation of reliable CSA adjusted to each plant fibre species [36]. Based on a sensitivity analysis, Islam et al. [32] also highlighted the relative significance of input quantities (fibre diameter, misalignment, etc) on the calculated fibre strength, and showed the significant influence of the gauge length.

Additionally, only few fibres have a stress-strain curve that is linear throughout the loading curve. For flax and hemp fibres, the literature generally reports three types of behaviour [40–43]. The first type (referred to as 'Type 1') is characterized by a truly linear response. The second type ('Type 2') shows non-linearity with a reduction in the apparent tangent modulus beyond an initial yield point. The third type ('Type 3') presents multiple non-linearities. In this case, the initial portion appears linear until a yield level is reached, after which a significant decrease in the apparent tangent modulus is observed. Subsequently, a second yield point emerges at a higher strain, followed by a slightly parabolic increase in the apparent tangent modulus until final failure. The origin of this complex non-linear behaviour remains a subject of debate in the literature and is attributed to partial microstructural rearrangements within the fibre cell walls [44–48]. It also complicates the determination of a longitudinal Young's modulus since the recorded apparent tangent modulus evolves during loading, even before plastic or damage events. While the initial stage of most tested fibres is generally linear, the limited strain range for some curves, along with the signal-to-noise ratio, renders sometimes the determination of the modulus

challenging in this region. Some standards recommend the use of the final stage of the tensile test, i.e., just before failure, to determine an apparent Young's modulus. However, this approach may not be practically meaningful, as fibres may have been damaged, and materials and structures are typically not likely to stress fibres to such extremes.

Finally, the fibre tensile strain cannot be obtained directly from its initial gauge length and displacement due to the slack in the specimen, slipping/seating in the grips [49] and to the compliance of the fibre mounting system (glue, load frame, load sensor) [22,49–51], defined as the inverse of its stiffness and introduced in ASTM C1557 and NF T25-501-2 standards [25,27]. Engelbrecht-Wiggans and Forster [49] demonstrated recently that the methods provided by the standards for strain corrections are not generically valid for single fibres that exhibit nonlinearity.

It is also worth noting that the sources of uncertainty are numerous and can be classified into categories. A classification into epistemic and stochastic or aleatory uncertainties is now widely accepted [52]. Epistemic uncertainty is due to a lack of knowledge and can therefore be reduced. Stochastic uncertainty arises from the inherent randomness of the objects of study and cannot therefore be reduced. This distinction is particularly useful for identifying sources of epistemic uncertainty that can be reduced. This is the challenge and interest of the present round-robin study.

Thus, the present interlaboratory experimental campaign aims at (i) better understanding and quantifying the sources of variabilities recorded while estimating the tensile properties of organic (synthetic and natural) fibres, (ii) proposing some useful recommendations to better analyse the tensile results in future fibre characterizations. For that purpose, three batches of fibres were selected, i.e., combed hemp and flax fibres as well as aramid fibres. Flax and hemp fibres were selected due to their prevalence among European fibre plants and extensive use in both textile and composite sectors. Alongside these natural fibres, aramid was selected as a synthetic fibre with dimensions and stiffness properties similar to those of the chosen plant fibres. The selection was also based on their shared similarities in microstructural organization and mechanical behaviour.

Experimental characterizations were performed by nine research groups using their own mechanical testing equipment and procedures, both for the CSA (and thus stress) and strain measurements. Individual elementary fibres were tested using single fibre tensile test. Specific data processing protocols are then developed to treat all data sets in the same way. Mechanical results are then compared and discussed, according to the type of fibre and method used.

2. Materials and methods

2.1 Fibres

In this study, we focused on the analysis of three distinct types of fibres: flax, hemp and aramid. For flax and hemp, scutched and hackled fibres were used. These fibres were extracted using the scutching and hackling facilities of Terre de Lin (Saint-Pierre-Le-Vigier, France). The flax fibres were obtained from Bolchoï variety plants (Terre de Lin) cultivated in Normandie (France) in 2018, while the hemp fibres were extracted from Futura 75 variety plants (Hemp-It) cultivated in Piacenza (Italy) in 2018 too. The high-performance K29 para-aramid fibres were produced by Dupont ™. They belong to the original family of Kevlar® product types.

Fibres from each type were supplied to all nine laboratories participating in this benchmark exercise. Figure 1 displays typical SEM, light optical and X-ray microtomography micrographs of the different fibres, depicting the intricate morphology and microstructure of the selected organic fibres. This figure shows that flax and hemp fibres exhibit a ribbon-like shape and irregular cross sections with open lumens (i.e. lumens that have not disappeared due to the collapse of the cell wall). In addition, these fibres show a pronounced roughness characterised by the presence of dangling fibrils and middle lamellae or cortical residue fragments on their surface. Thanks to the high spatial resolution of the SEM images, it is also possible to distinguish the presence of kinks distributed all along the length of the flax fibre. In contrast, the aramid fibres are more regular and straighter and have circular cross sections with a smaller diameter.

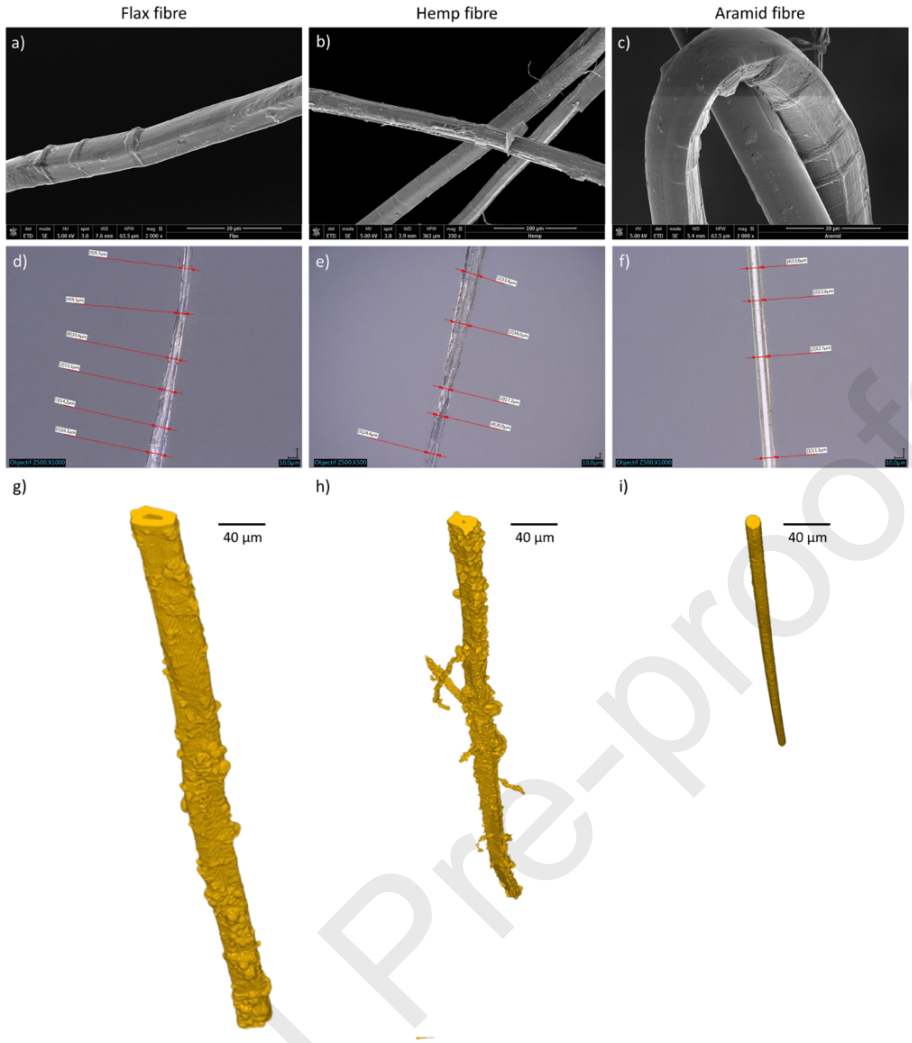

Figure 1: (a-c) SEM and (d-f) light optical micrographs of flax, hemp and aramid fibres. (g-i) 3D-rendered perspective views (voxel size: 0.35³ µm³) of the three types of fibres obtained using synchrotron X-ray microtomography (BM05 beamline, ESRF, Grenoble, France).

2.2 Experimental methods

Individual elementary fibres were used for the single fibre tensile tests. The fibre selection, individualisation into single fibres, preparation, morphological characterisation and tensile testing were carried out following the typical procedures, methods, and equipment used in the different participating laboratories. When launching the benchmark, a specific protocol (provided in supplementary information, SI1) was given to all participating laboratories. It details the recommendations for fibre preparation and conditioning, mounting conditions (paper cardboard), gauge length (10 or 12 mm), displacement rate (1 mm/min) during the tensile test, the number of fibres to be tested, data acquisition conditions (force and displacement/strain, relative humidity, temperature) and data processing. However, due to differences in available equipment, some adaptations were necessary in certain cases. Table SI-1 in SI2 lists the laboratories that participated in the benchmark exercise (labels assigned to each laboratory will be used in the remainder of the study exclusively to streamline the presentation and discussion of the results). Table SI-2 (SI2) provides a concise summary of the experimental procedures and parameters effectively employed by the different laboratories in this benchmark exercise. For flax and hemp, fibres having apparent diameters higher than 30 µm and 40 µm were excluded for the analysis considering the high probability of being constituted of multiple elementary fibres.

2.3 Data post-processing and statistical analysis

The post-processing of the raw data, i.e. apparent fibre diameter, displacement and force, involved multiple analysing steps. Initially, post-processing was conducted using methods employed by each research group. However, a first comparison of the results revealed significant discrepancies, attributed in a first instance to variations in the protocols used to determine tensile properties and to factors related to non-linearity in the mechanical response of the fibres, such as methods for determining the E-modulus, considered strain range, and corrections for machine compliance or the foot of the force-displacement curve (slacks in fibre and load train, see SI1). Subsequently, a precise data processing protocol, described in Figure SI-1 (SI2), was developed and adopted by the entire consortium. Collected data were then analysed by each partner following this protocol (PTP: Partner Post-Treatment). Additionally, the data processing protocol was implemented in MATLAB (PTU: Unified Post-Treatment), the raw data were then processed by Lab C to assess the impact of protocol implementation. An initial apparent tangent modulus (Ei) and a final apparent tangent modulus (Ef) were determined using two different strain ranges (between 0.05% and 0.5 % for Ei and between ε_{max} -0.2% and ε_{max} for Ef) as described in Figure SI-1 (SI2). Stress and strain are presented using engineering stress and engineering strain. The stress and strain at failure (σ_R and ε_R) were determined by looking for a 30% drop in stress. The preceding data point before this drop delineates the stress and strain at failure.

The raw data and all the details regarding the experimental set-up and protocol from all the partners were collected following a specific notice (see instruction manual for the completion of data collection files in SI3). Statistical tests were used to assess whether the determined tensile properties for each fibre type across the different laboratories significantly differ from each other. Initially, a one-way ANOVA (Analysis of Variance) test was applied for each fibre type for the different laboratories to check whether there was a significant difference between at least two groups, although it does not specify which groups differ. Subsequently, a post-hoc test, namely Tukey's range test, was used to determine, through multiple comparisons, whether significant variations existed in the mean results among them. This approach allows for the identification of not just one, but several groups that are significantly different from each other. For each property and each laboratory, a letter is assigned. Different letters indicate that the configurations are statistically different.

3. Results and discussion

3.1 Determination of the CSA

Boxplots of the cross-section areas determined by the different laboratories, for the three tested fibre types, are shown in Figure 2, row a. All the values are summarized in Supplementary Information, SI2 (Table SI-3, Table SI-4 and Table SI-5). A synthetic version of the table, giving the values of the mean, standard deviation, coefficient of variation as well as the letters from the Tukey's test is also proposed in Table 1. Noticeable variations in the median values and the distribution of the CSA can be observed across laboratories. The median value of the CSA ranges from 90 μm^2 to 134 μm^2 for K29 aramid fibres (SI2, Table SI-3). According to the technical datasheet provided by the supplier, aramid fibres have a nominal diameter of 12 µm, which corresponds to a cross-sectional area of 113 μm^2 assuming a perfectly circular cross-section. However, it is worth noting that literature sometimes reports variations in the measured fibre diameter [37,53,54]. In the present study, the median values measured by the laboratories (inter-laboratory variability) differ by approximately plus or minus 20% compared to this nominal value. These discrepancies are attributed to errors related to apparent diameter measurements, which can be associated with factors such as optical focusing, distortion and calibration of diameter measuring devices.

The inter-laboratory variability is even more pronounced for flax and hemp fibres. The median value of the cross-sectional area ranges from 68 μm^2 to 441 μm^2 for flax (SI2, Table SI-4) and from 105 μm^2 to 897 μm^2 for hemp (SI2, Table SI-5). It is noteworthy that these fibres exhibit irregular and non-uniform cross-sectional geometries, displaying variations along their length and between individual fibres. This is even more pronounced in the case of fibre bundles [36]. Therefore, in addition to differences in measurement techniques, tools and protocols, inter-laboratory variability is also influenced by the fibre selection bias. For example, for flax, it is possible to note that the CSA measured by laboratories B and D (with mean values of 429μm^2 and 369 μm^2, respectively, see Table 1) are almost double of the mean value determined from all the data (233 μm^2). The size of the selected and isolated plant fibres indeed closely depends on the dexterity and experience of the operator. This can result in batches of tested fibres with significantly different CSA, as observed in the present study.

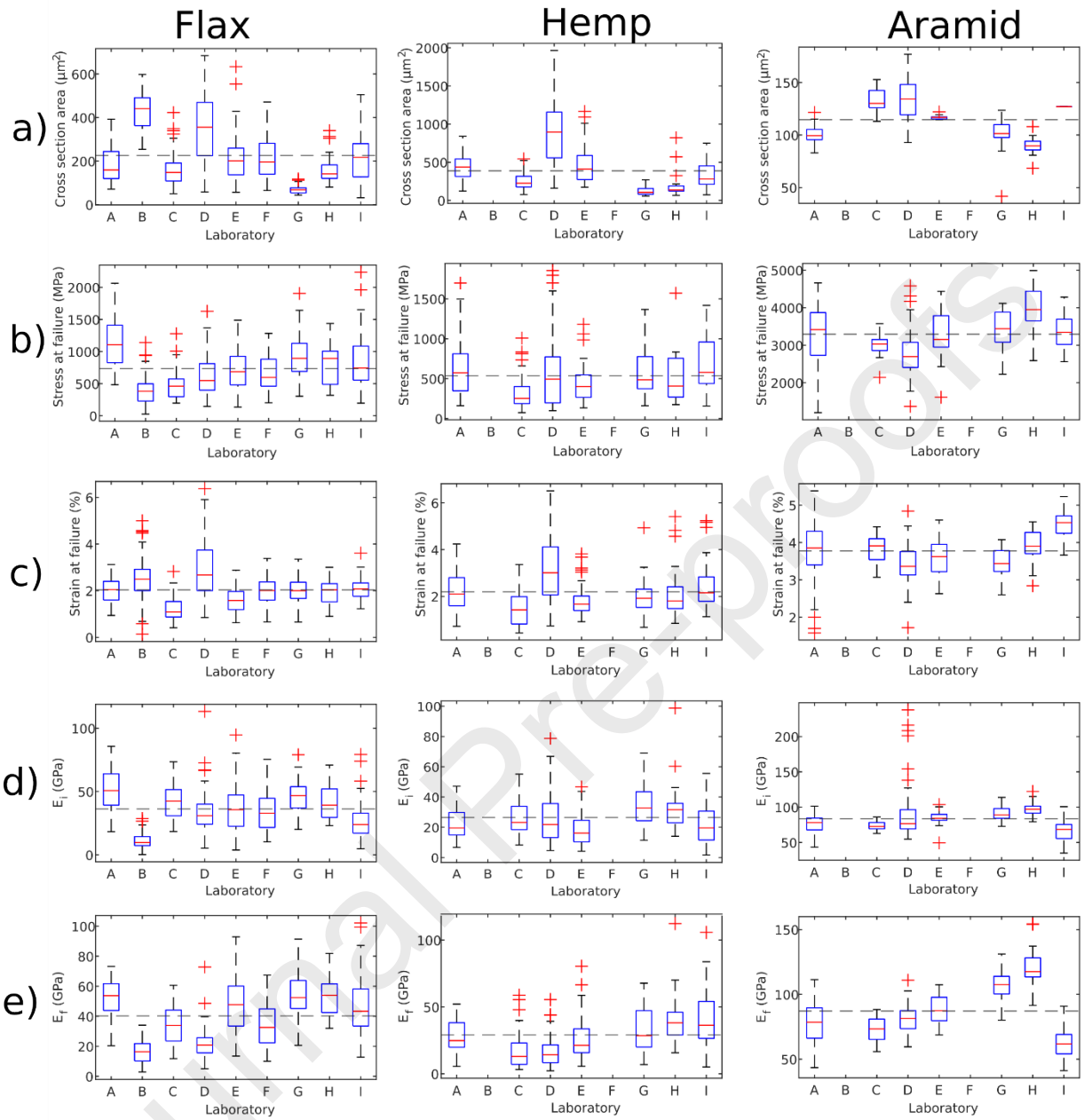

Figure 2: Box-plots of the cross-section areas and tensile properties determined (rows) by the different laboratories for the three tested fibres types (columns). In the box plots, the central mark represents the median value, while the lower and upper edges of the box denote the 25th and 75th percentiles, respectively. The whiskers extend to the most extreme data points that are not considered outliers, and any outliers are individually plotted using the '+' marker symbol. By default, an outlier is defined as a value that exceeds 1.5 times the interquartile range above or below the top or bottom of the box. The horizontal dotted line represents the overall mean value calculated from all experimental data.

Table 1: Average experimental tensile properties determined from each laboratory (mean value ± standard deviation (CoV) and significance letters from the Tukey's statistical analysis)

Cross section area (μm²)				
Stress at failure (MPa)				
Strain at failure (%)				
Initial modulus Ei (GPa)				
Final modulus Ef (GPa)				

One of the key influential factors also lies in the application of different geometrical models (e.g. circular vs. elliptical) to determine the CSA. Based on the dataset of laboratory A equipped with an automated laser scanning apparatus, the decrease in CSA when considering an elliptical model instead of a circular one for the determination of the CSA is –2.9 %, -11.8% and –27.1% for aramid, flax and hemp elementary fibres, respectively. This has to be related with their respective cross-sectional shape factor of 1.24, 1.63 and 2.21, respectively, which obviously has a greater impact the higher it is [36,39], and on the choice of the geometrical model for determining CSA. It should also be pointed out that, given the hygroscopic nature of plant fibres, the CSA can undergo variations according to moisture content. Therefore, the relative humidity, even if sometimes different between laboratories, was carefully controlled in this benchmark study, and CSA measurements were conducted under the specific hygrothermal conditions intended for subsequent tensile testing.

Furthermore, when examining the discrepancies for each laboratory, i.e. intra-laboratory variability, it can be observed that the scattering is significantly smaller for aramid fibres with a coefficient of variation (CoV) only ranging between 2% and 14%. In contrast, the CoV varies between 20% and 57 % for flax fibres and between 40% and 94 % for hemp fibres, reflecting the more significant variations probably induced by the extraction/isolation protocol of the fibres as well as the irregularity, the non-uniformity and the spatial variation of their morphology. These values also illustrate the greater morphological variability among hemp fibres compared to flax, a fact already documented in the literature [36], which can be also attributed to the greater difficulty to extract and isolate elementary hemp fibres due to more cohesive and lignified bundles.

3.2 Tensile curves

Figure 3 illustrates the stress-strain curves obtained for the three types of fibres tested by Laboratory E. It includes approximately 50 to 70 fibres of each type. Even if some scatter is evident in the stress–strain curves, the range covered by the group of curves is narrower for aramid fibres (Fig. 3c) compared to flax (Fig. 3a) and hemp (Fig. 3b) fibres. Single fibre tests are dispersive in nature, influenced by inherent material features like microstructural variations, defects, and voids within the fibre (Fig. 1), along with measurement uncertainties. All the tested fibres exhibit very limited or non-existent plastic behaviour. Interestingly, aramid fibres show an even distribution of moderate non-linear behaviour, as previously reported [55]. In contrast, flax and hemp display a range of tensile curve shapes, including linear behaviour as well as various non-linear patterns, as previously observed and mentioned in this manuscript.

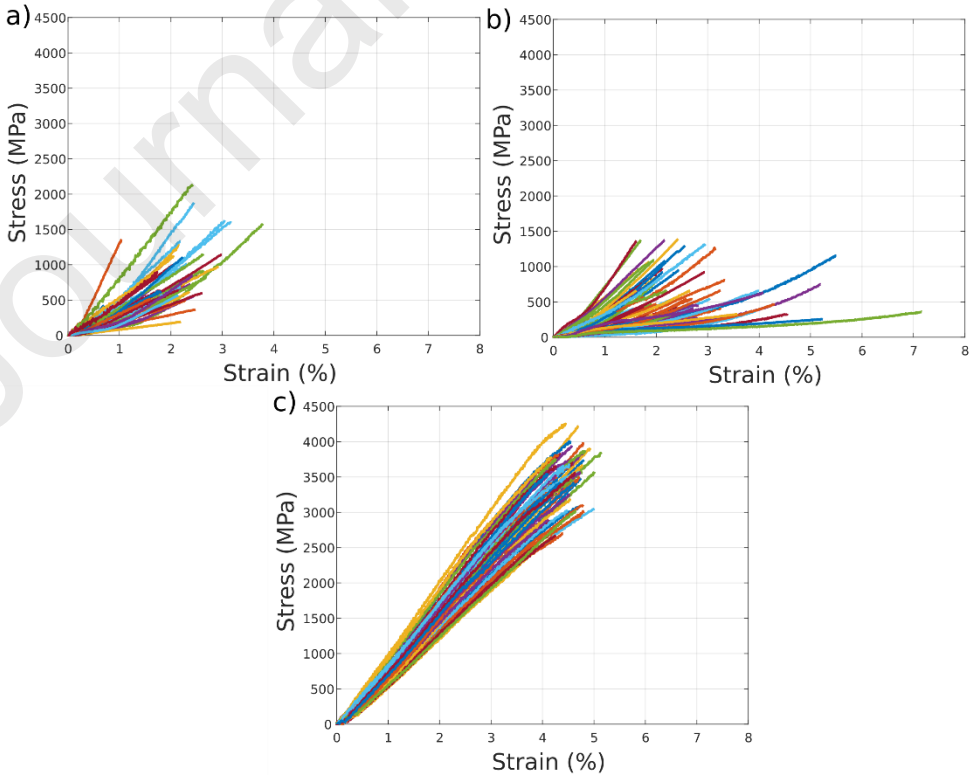

Figure 3: Stress-strain curves collected by laboratory I for flax fibres (a), hemp fibres (b) and aramid fibres (c).

Figure 4 displays the stress-strain curves produced by the different participating laboratories for the three types of fibres. Across all laboratories (except Lab D), a consistent conclusion can be drawn regarding the narrower envelope observed for aramid fibres. However, it is evident that the range levels and areas covered by the group of curves vary from one laboratory to another. This highlights the significant impact of testing practices and parameters on the dispersion of results.

The plots also highlight the differences in data recording practices and offsetting, which are closely tied to the functionalities offered by commercial tensile testing equipment. Some laboratories begin recording data when the tensile force becomes effective, which means that the displacement required to eliminate the slacks in fibre and load train is not recorded (laboratories F, G and H, for example, described as “test starts directly” in Fig. SI-1 of SI2). In contrast, others record from the pre-loading phase (described as “test starts by a plateau” in Fig. SI-1). Regardless of the chosen approach, the critical aspect is to establish the zero load and zero displacement correctly. Any inaccuracy in these settings has a direct impact on the determination of the tensile properties. As described in Fig. SI-1 (SI2), three specific treatments have been applied to obtain a homogenous set of data, whatever the approach of each research group.

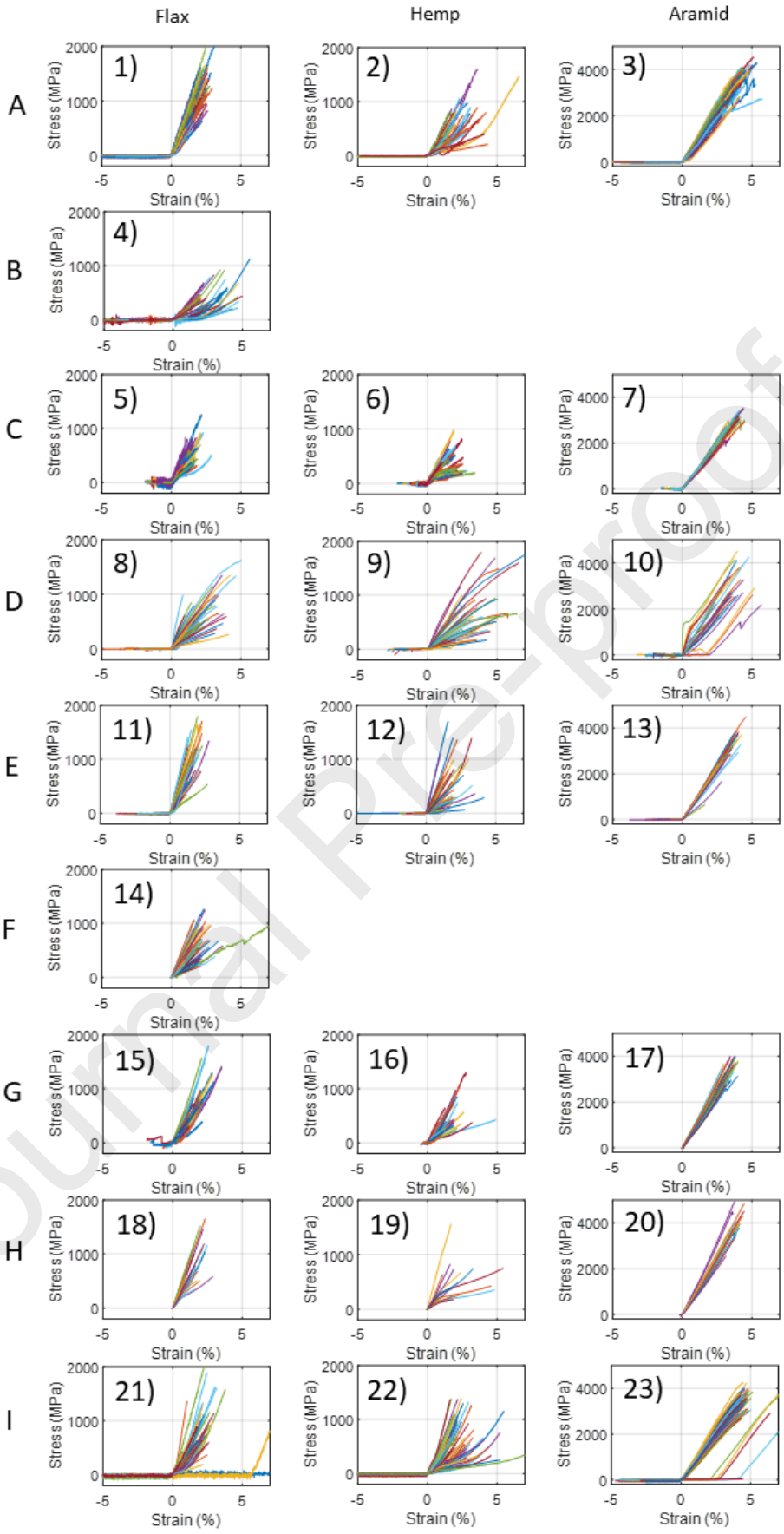

Figure 4: Stress-strain curves collected by the different laboratories and fibres types. The load frame compliance is corrected.

Occasionally, a sudden drop in load appears on the curves before failure (Fig. 4). This could be attributed to slippage in the clamping area, partial fibre failure, or a failure event when testing a small bundle of fibres inadvertently. Initially, we advised rejecting these curves during the post-processing stage. However, subsequent results revealed that this issue is limited to only a small number of curves, and for our study, the rejection does not significantly alter the mean and standard deviation values. Consequently, the decision was made to include all curves in the post-processing phase (PTU). The number of fibres prepared, tested and post-treated for each laboratory and fibre type is given in Table SI-2 (SI2). The variations in numbers among these different categories is related to the occurrence of fibre breakage during preparation, handling, mounting and gripping.

3.3 Tensile properties

Both intra- and inter-laboratory variabilities are also noticeable in the tensile modulus, strength and strain at failure of the different fibres. This is evidenced by the boxplots of Figure 2, in Table 1, in tables in SI2 and in Figure 5, which shows cumulative distribution curves for all the measured tensile properties and laboratories.

- **Inter-laboratory variability**

The median values for the initial (Ei) and final (Ef) apparent tangent tensile moduli fall respectively within the range 68-97 GPa and 62-118 GPa for aramid fibres, 10-51 GPa and 16-54 GPa for flax fibres and 16-33 GPa and 13-38 GPa for hemp fibres. For tensile strength, the median values range from 2821 MPa to 3981 MPa for aramid fibres, 383 MPa to 1107 MPa for flax fibres and 252 MPa to 577 MPa for hemp fibres. Finally, concerning strain at failure, the median values range from 3.4% to 4.5% for aramid fibres, 1.2% to 2.9% for flax fibres and 1.4% to 3% for hemp fibres. The significance letters derived from the Tukey's test (presented in Table 1) indicate statistically significant variations between the mean values of the tensile properties across the different laboratories for hemp and flax fibres. Comparatively fewer significant differences are noted among the means for aramid fibres.

Table 1 provides also the average tensile properties calculated from all the fibres successfully tested by the nine laboratories (286 fibres for aramid, 454 for flax and 321 for hemp). The mean values of Ei, Ef, σ_R and ε_R are equal to 80.3 GPa, 81.1 GPa, 3264 MPa and 3.86% for aramid fibres, 36.1 GPa, 38.7 GPa, 719 MPa and 2% for flax, and 25 GPa, 27.4 GPa, 529 MPa and 2.17% for hemp.

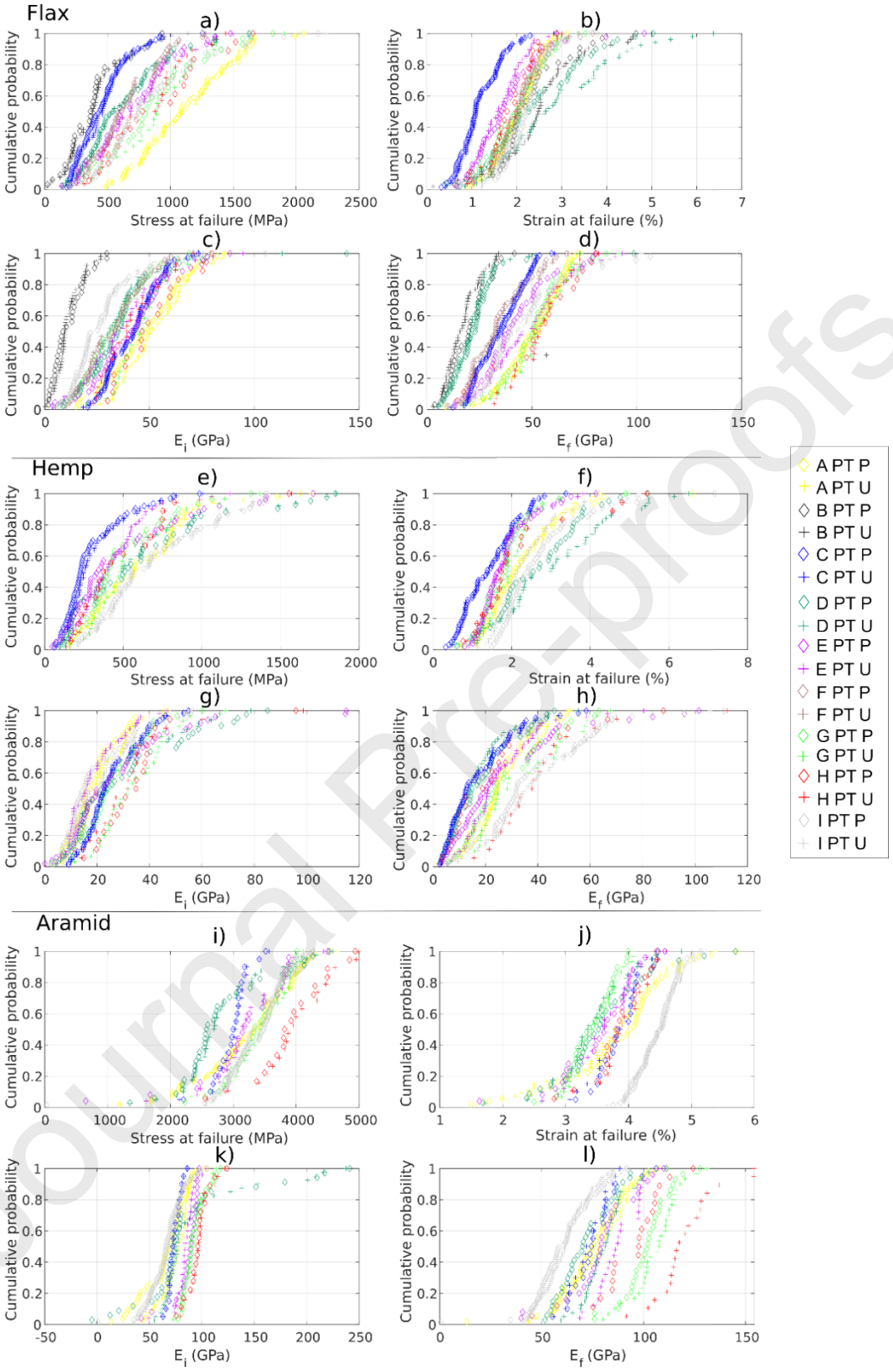

Figure 5: Cumulative distribution curves of the tensile properties determined by the different laboratories for the three tested fibre types. The marker colours in the plots correspond to the different analysis laboratories, while the marker shapes represent the data post-processing methods. Specifically, 'P' stands for post-processing conducted by each individual laboratory, and 'U' signifies standardized post-processing.

In literature the ranges reported for the Young's modulus, tensile stress and strain at failure are 37.2 – 75.1 GPa, 595 – 1510 MPa and 1.6 – 3.6% for flax and 14.4 – 44.5 GPa, 285 – 889 MPa and 0.8 – 3.3% for hemp [56].

The values obtained in this study are therefore on the lower end for flax and in the mid-range for hemp, considering that most literature data for hemp are for fibres processed with hammer milling systems and not through scutching, as in our study. For aramid, the mean values measured in our study are in good agreement with the tensile modulus, strength and strain at failure mean values (± standard deviation) of 78.1 ±9.6 GPa, 3 300 ±500 MPa and 3.8 ±0.3%, respectively, reported in [53] for K29 fibres.

For flax, the CoV of these properties calculated from all data (see Table 1) are around 50% for the moduli and strength and 40% for the strain at failure. The values are around 60% and 50% for hemp. These values are slightly higher than those typically reported in the literature with CoV values between 25 and 38% for the tensile properties of flax and between 33.3 and 46.2% for hemp [57], considering that the literature data have been systematically determined by a single laboratory. The lower variability in strain at failure, compared to other tensile properties, is attributed to its independence from the measurement of the effective CSA and the associated high uncertainties. For aramid fibres, the CoV is around 30% for the moduli and slightly lower than 20% for the stress and strain at failures. This can be compared to the CoV of 12.3%, 15% and 7.9% for the same quantities extracted from [53].

The overall reduction in variability for aramid, compared to flax and hemp, clearly highlights the significant influence of the complex morphology of plant fibres on measurement errors and uncertainties. In materials science, and for characterization techniques with limited measurement uncertainties, a greater dispersion in failure properties is generally observed or expected compared to stiffness. Indeed, failure behaviour is more sensitive to defects. Obtaining a higher variability for the stiffness of aramid fibres highlights the significance of the nonlinearity of the tensile response in determining the modulus.

It is also noteworthy that there is greater degree of variability among the results obtained from the nine laboratories for plant fibres compared to aramid fibres. Variations in the mean values from each laboratory compared to the overall mean calculated from all experimental data for Ei, σ_R, and ε_R are -15%/+21%, -17%/+21% and -12%/+17% for aramid, -34%/+41% (excluding- partner B which as an outlier value of 72%), -47%/+54% and -45%/+35% for flax and -36%/+32%, -52%/+9% and -35%/+38% for hemp. For the apparent modulus and strength, this discrepancy is attributed to the greater challenge in determining the effective CSA of plant fibres due to the complexity of their morphology. Additionally, their nonlinear behaviour is more pronounced compared to aramid, which directly affects the determination of the apparent modulus.

Figure 5 also shows the influence of the data post-treatment protocol's implementation by comparing the results obtained using the partner's post-treatment (PTP) and the unified data post-treatment (PTU) implemented in MATLAB® by Lab C for processing all the raw data. The differences between the results obtained with two post-treatment protocols are generally minor, except for the final modulus for some of the partners, as seen in e.g. Laboratory H for aramid. This suggests that when the data post-processing protocol is rigorously defined and implemented, it exhibits a limited impact on the determined properties. The observed discrepancies are typically associated with displacement offsetting and the detection of the fibre failure point, directly affecting ultimate tensile properties and hence the final modulus.

- **Intra-laboratory variability**

For Ei, the CoV of the initial apparent tangent modulus, for each laboratory, spans from 8% to 22% for aramid fibres (except for Lab D, which exhibits a value reaching 48%, but with disturbances evident in some of the stress-strain curves, see Fig. 4. 10), 28% to 54% for flax fibres and 38% to 68% for hemp fibres while the CoV of the final apparent tangent modulus ranges from 11% to 19%, 24% to 51% and 49% to 74% for these respective fibre types. This significant intra-laboratory variability is strongly related to the high uncertainties in CSA measurements, which is significantly larger for plant fibres than for aramid fibres. The other main sources of variability originate from the correction of the compliance of the testing system and from the non-linearity of the responses of some tested fibres and the variability of the non-linear patterns observed, strongly related to the crystalline cellulose microfibril angle in the cell walls of plant fibres. The slight increase in the Ef modulus observed for most of the laboratories, compared to the initial modulus Ei, can be attributed to microstructural rearrangements within the fibres induced by the tensile and shear stresses.

For the stress at failure, intra-laboratory variability, primarily arising from uncertainties in the CSA measurements, is significantly lower for aramid fibres (with CoV ranging from 10 to 23%) compared to flax fibres (CoV ranging from 32 to 59%) and hemp fibres (CoV ranging from 51 to 80%). In each laboratory, the distribution

of strength correlates with flaw sensitivity. These defects can be inherent to the fibres themselves, originating from their production and transformation processes, or introduced during fibre preparation and handling for testing. Additionally, multiaxial stress concentrations near the fibre ends within the gauge section, resulting from clamping and/or misalignment and/or geometrical variations, can also lead to premature failure.
For the strain at failure, the CoV range from 8% to 23% for aramid fibres, 23% to 44% for flax fibres and 36% to 58% for hemp fibres. In this case, another source of inter-laboratory variability is associated with the method used to measure the global displacement of the fibre as well as the correction of the compliance of the testing system (see Table SI-2).

Globally, these CoV values are slightly higher than those reported in the literature and mentioned in the previous paragraph. However, it is important to consider the number of fibres tested in each batch when comparing these values to literature ones.

- **Comparison with IFBT**

Finally, these tensile properties and scattering obtained from single fibre tensile test can be compared with those obtained in literature using IFBT. Interestingly, for flax, a round robin test has already been organised and results are published in reference [6]. The properties of scutched and hackled flax fibres (*Aramis* variety) were determined by 5 laboratories using IFBT. The back-calculated fibre stiffnesses, E1 measured between 0 and 0.1% strain and E2 determined on 0.3 -0.5 % of strain, ranged between 57.5 and 63.3 GPa and 36.6 and 46.1 GPa, respectively. It shows a scatter between the five laboratories of less than ±5% when compared to the average values measured from all the experimental data which are equal to 59.8 and 40.8 GPa, respectively. This is significantly lower than the inter-laboratory variability observed in the present study when using single fibre tensile test (see the "inter-laboratory variability" sub-section). The intra-laboratory variability is also lower with CoV values roughly comprised between 7.5 and 15%. In IFBT, a large quantity of fibres is tested simultaneously, thus providing a homogenization effect and an averaged response for each tested sample, explaining the lower scattering when compared to single fibre tensile testing.

For the tensile strength, the average values back-calculated by the five laboratories are comprised between 341 and 667 MPa, showing a higher scatter of approximately ±30% (the average value calculated form all the experimental data being 527 MPa). Regarding the intra-laboratory variability, the CoV values are approximately ranged between 10 and 30%. This higher scatter, compared to stiffness values, was attributed by the authors to the fact that this property is highly sensitive to imperfections and flaws. This level of dispersion, although lower than that observed in the present study on single fibre tensile test, is nevertheless of the same order of magnitude.

Interestingly, it can be observed that the average values of the tensile strength are higher and the stiffness lower for single fibre tensile tests compared to IFBT. However, it is necessary to note that the same flax fibres were not tested in both studies. In IFBT, both individual fibres and bundles of fibres are tested, and it is known that bundles exhibit lower strength than individual fibres. Moreover, the composite tensile strength is also greatly influenced by the quality of the fibre-matrix interface, the fibre division and also the possible presence of woody core, cortical parenchyma or middle lamellae residues. The failure modes may also differ in the two types of tests. In particular for IFBT, the results depend on the fibre-matrix interfacial bonding, and also on the fibre individualisation and spatial distribution in the resin. By averaging results across a large number of fibres, the IFBT method focuses on the mean value and does not allow for determining the probability distribution.

For long aligned hemp fibres, Gabrion et al. [58] reported average values obtained through IFBT tests comprised between 45 and 64.3 GPa for E1 (determined on 0-0.1% of strain) and between 21.5 and 43.2 GPa for E2 (determined on 0.3 -0.5 % of strain) for different varieties, agronomic conditions and processing parameters. The average strength ranges between 318 and 616 MPa. The CoV varies between 2.3 and 18.4% for E1, 1.2 and 17.3% for E2 and 2.3% and 21.6% for the tensile strength. Again, for hemp, IFBT leads to higher modulus and lower/similar strength and shows much less scatter than single fibre testing.

3.4 Recommendations and guidelines for best practices and standardization

In view of the results obtained in this inter-laboratory round-robin study, Figure SI-2 (SI2) presents a mind-map that comprehensively outlines the experimental and analysis steps, key testing parameters, and all points of

caution related to “a proper” execution of a tensile test on single fibres. These different key factors are categorized by families such as e.g. preparation, conditioning, stress and strain measurements. The results and experience gained during this benchmark exercise provide insights into potential areas for improvement, as detailed below.

- **Fibre morphology and cross-sectional area**

The results demonstrate the predominant influence of the effective cross-section of the fibre (and its spatial variation along the gauge length) on its tensile properties. For plant fibres, it is essential to accurately identify the geometry and internal structure of the object, especially whether the fibre is single or multiple; the considered element (fibre or bundle) must be carefully indicated to avoid any confusion. The use of non-destructive techniques with high spatial resolution, allowing access to the internal structure of the fibre, is recommended. Finally, if the goal is to identify the properties of the fibre’s cell wall rather than the apparent properties of the fibre, it is necessary to take the fibre lumen into account to assess the actual strengthen cross-section. X-ray microtomography is a well-suited technique for the 3D morphological characterization of these small, complex-morphology objects. However, the cost and time required for such experiments are not compatible with campaigns involving testing hundreds of fibres.

- **Sample preparation, mounting and clamping**

In this work, the fibre alignment was visually controlled. To further reduce the inaccuracies in the gauge length, limit the multiaxial stress concentrations near the fibre ends within the gauge section and the possible premature failure of the fibre, it is recommended to carefully check the alignment of the testing machine prior conducting tests, measure and consider alignment defects when calculating tensile properties. Incorporating multi-axial force sensors and actuators into the tensile machine could also enable the adjustment of fibre alignment upon testing. Another approach to minimize the stress concentration factor at the exit of the jaws undoubtedly lies in the design of new grippers.

- **Environmental conditions**

When it comes to characterizing and comparing the morphological and mechanical properties of fibres, precise control of hygrothermal conditions is required to limit errors caused by dimensional variations induced by laboratory environmental fluctuations [59], as well as softening effects which considerably influence tensile properties, especially for plant fibres [51,60]. Indeed, due to the specific structure, high structural anisotropy and hygroscopy of plant fibres, the humidity level can strongly impact the fibre diameter and cross-sectional shape. In particular, an important swelling is noticed at high relative humidity (RH), inducing significant variations in diameter and CSA, e.g. cross-sectional hygroexpansion coefficients ranging from 0.42 to 1.70 have been measured for plant fibre bundles at 20-73 %RH [61], a radial hygroexpansion coefficient of 1.14 has been found for elementary flax fibres at 20-98 %RH [62]. In this benchmark study, the variation in RH conditions between the different laboratories was rather limited (38-65% RH, see Table SI-2), ensuring good comparability of results.

- **Sampling**

The number of fibres to be tested should be determined based on the inherent variability of each fibre type. This study has shown higher levels of dispersion for flax than for aramid, and even higher for hemp. So, it is evident that a testing campaign for plant fibres should include a larger number of tests, compared to synthetic fibres. The sampling can be refined using uncertainty quantification methods such as bootstrap methods [63]. It was found that for batches of around thirty aramid fibres, halving the amplitude of the confidence interval requires multiplying the sample size by 4 (2^2). Dividing the amplitude by three would require a 9-fold increase in sample size (3^2). For carbon fibres, Mesquita et al. [64] indicated that a high number of tests (over ~ 200) is necessary for accurate determination of the fibre strength Weibull parameters; showing that samplings of ~ 50 tests can lead to a Weibull modulus deviation of ±1. It is also very useful to specify the number of tested fibres and the number of fibres and results (either morphological or mechanical) discarded from the analysis, as given in Table SI-2 of this study. A high number of rejected tests could be an indicator of the operator dexterity but also of the batch homogeneity. It is also worth noting that the extraction of fibres during their preparation for single elementary fibre testing can cause damage, and a selection bias may be induced by the fact that the weakest fibres may not be handable and testable.

- **Strain measurement and compliance**

When the fibre strain is determined from the global displacement of the tensile set-up, the compliance correction is highly recommended. In fact, based on calculations detailed in standard NF T25-501-2 [27], e.g. for a system compliance of 0.2 mm/N, the E-moduli of elementary flax fibres of 12 mm long, 15 µm in diameter, with apparent E-moduli of 16-54 GPa will be increased up to 16.8-64.2 GPa, the correction applied can thus reach several tens of percent. When the compliance of the tensile system was determined (see Table SI-2 for details of the compliance values found by the laboratories), the E-modulus and strain at failures values measured in this work were therefore corrected accordingly. However, as recently reported [49], the development of new compliance determination protocols is necessary to account for the possible variation of the machine compliance depending on the fibre type and as a function of the load level [65]. It is also essential to account for gripping movements in displacement measurements, consider pre-load (the load required to align the fibre with the loading axis and to remove slack in the drivetrain) and include the corresponding displacement when determining the initial gauge length. While there is no universal best method, the key is to describe the procedure meticulously and apply it consistently to all the fibres tested. It should be pointed out that recording data during the preloading phase enables access to all data and facilitates their further post-processing.

While it may be challenging and time-consuming, it is desirable that in the future, direct strain measurements (using particle tracking or more sophisticated methods such as digital image stereo-correlation or other advanced technologies) would be favoured over displacement-based measurement approaches. These methods will provide a more accurate measurement of strain and can also provide information about the heterogeneity of the displacement field over the length of the fibre.

- **Apparent modulus determination**

Based on the results obtained in this study, and as recently highlighted by Engelbrecht-Wiggans and Forster [49], it is advised against relying solely on linear regression over the final points of the stress-strain curve to determine the tangent apparent modulus. Instead, this method should be employed cautiously and primarily for the purpose of comparison.

- **Fibre strength**

It is crucial to precisely define the type of object under testing, i.e. single fibre or fibre bundles and its processing (scutching, hackling, stretching…), as well as the concept of failure and the corresponding method for detecting failure and determining failure stress.

- **Data acquisition and post-processing**

Beyond the need for a very detailed description of the post-processing of all published data on fibre properties, this study revealed that it is preferable to use high data acquisition frequencies (values to be defined according to the displacement rate), and start data acquisition from the early stages of pre-loading. This allows a more precise determination of force and displacement zero points, as well as the fibre failure point. These parameters are likely to have a significant influence on the determination of the tensile properties.

- **Purpose of the single fibre tensile tests**

Finally, a critical question undoubtedly concerns the purpose of the single fibre tensile tests. If the goal is to access the intrinsic properties of the fibres, as for many applications for textile and fibrous media, or for understanding the behaviour of isolated fibres, the tensile test on single fibre is definitely recommended, especially if a link is done with ultrastructural characterization such as local biochemical or mechanical analysis, micro-CT or microscopy. This is also particularly relevant when dealing with recycled fibres, given the variability in fibre lengths. Considering the influence of fibre length (or volume) on strength, a test that evaluates all fibres simultaneously fails to acknowledge this dependency.

If the aim is to determine, e.g. the reinforcement potential of these fibres for composite applications, the issue of gauge length and boundary conditions must be raised to ensure that the measured properties are representative of those of the fibre in its final application. It should also be borne in mind that fibres morphology, and in particular their cross-sectional shape or lumen size, can potentially change in the composite compared to raw fibres, due to fibre collapse or resin filling. This can lead to significant variations between apparent fibre

mechanical properties, when determined on isolated fibres or by back-calculation approaches such as the IFBT method. Shah et al. [7] have previously highlighted the significant disparities between fibre properties obtained through single fibre tests and those back-calculated using IFBT. They underlined that these differences result from errors and inherent measurement issues in each method. If they have identified, as in the present study, various sources of error in single fibre testing (such as error in CSA, strain range for stiffness determination, differences in elementary and technical fibre properties and gauge length during single plant fibre tests), it is crucial to acknowledge that sources of error also exist for IFBT. The likely origins relate to errors in predictions based on the rule of mixture. Despite numerous factors contributing to error, such as misorientations in reinforcement, processing history effects, and the not entirely elastic behaviour of plant fibres and their composites, the most significant point is certainly the non-uniform fibre properties which are stochastic in nature. This emphasizes the imperative need for accurately measuring the distribution laws of fibre properties.

This is especially critical for strength, as it is fundamentally governed by the distribution law of failure stresses.

In alignment with Shah et al.'s [7] conclusions, it is recommended to adopt a pragmatic approach by using composite samples (and IFBT tests) to determine effective fibre properties when pre-dimensioning composite materials and structures. This method efficiently provides average effective properties of fibres without selection bias and encompassing individual fibres and fibre bundles. It also has limitations. It does not allow the determination of the strain at failure of fibres and it only allows the determination of certain elastic parameters.

When it comes to high-end and optimized composite structures, it becomes imperative to employ sophisticated models and establish comprehensive design and dimensioning guidelines, as well as in-depth understanding of the nano- and micro-structural underpinnings influencing the macroscopic material behaviour. This knowledge is particularly crucial for the development of multiscale approaches and models capable of accurately predicting and reproducing macroscopic behaviours under complex (multi-axial, cyclic…) in-service solicitations. For such approach, it is highly desirable to consider data on matrix and fibre properties. Recent studies, using both on experimental approaches [57] and multi-scale stochastic modelling [66], have reassuringly shown that the significant variability at the fibre level does not necessarily propagate to the composite level. CoV drops from values sometimes exceeding 50% at the fibre scale to less than 10% at the composite scale. This reduction is due to epistemic uncertainties at the fibre level and to an averaging effect at the composite level. So, a significant challenge for the composite community in integrating plant fibres into high-end structural applications lies in minimizing the share of variability due to measurement uncertainties in single fibre testing. This effort aims to ensure that dispersion values predominantly reflect the intrinsic variability of fibre properties. Achieving this involves enhancing and widely adopting single fibre testing standards to harmonize practices and ensure better homogeneity and comparability of data in the literature, an objective to which this round-robin study aims to contribute.

4. Summary and conclusions

In this study, we examined the variability in tensile properties among three types of organic fibres—aramid, flax, and hemp—which exhibit non-linear behaviour and fairly brittle failure. A total of approximately 1250 fibres were tested by 9 research groups using single-fibre tests on elementary fibres. The quantity of fibres tested per laboratory and the number of laboratories involved far exceed those reported in previous interlaboratory exercises conducted on individual fibres tensile testing. Results highlighted significant intra- and inter-laboratory variabilities as summarized in Table 2.

Table 2: Ranges of median and CoV values for the tensile properties determined by each laboratory for the three types of fibre

Range of **median values** (*range of CoV values*)	**Ei (GPa)**	**Ef (GPa)**	**σ_R (MPa)**	**ε_R (%)**
Aramid	**68-97**	**62-118**	**2821-3981**	**3.4-4.5**

	(8-22%)	(11-19%)	(10-23%)	(8-23%)
Flax	**10-51** (28-54%)	**16-54** (24-51%)	**383-1107** (32-59%)	**1.2-2.9** (23-44%)
Hemp	**16-33** (38-68%)	**13-38** (49-77%)	**252-577** (51-80%)	**1.4-3** (36-58%)

Human factors (fibre selection and handling) and experimental procedures, especially for the estimation of the fibre cross-sectional area and the tensile strain, were identified as the main sources of scatter in tensile properties. Post-processing procedures, particularly determining the starting point of the tensile test, are crucial, involving the elimination of slacks in fibre and load trains. The more pronounced scatter for flax and hemp compared to aramid was attributed to the difficulty to analyse the high variability and complexity of plant fibre cross-section and the greater diversity of non-linearities observed on stress-strain curves.

The main recommendations for reducing dispersion in tensile testing include considering geometrical models adapted to fibre morphology when determining the cross-sectional area, maintaining precisely controlled hygrothermal conditions, ensuring consistency in controlled environments for both dimensional and mechanical characterization, accurately defining zero load and zero displacement points, and systematically specifying the strain range used to determine apparent tangent modulus. The use of the final part of the stress-strain curve is not recommended for the determination of the apparent tangent modulus. A critical point remains the verification of the unitary nature of the fibre. The use of non-destructive techniques with high spatial resolution, allowing access to the internal structure of the fibre, is recommended to rule out multiple fibres. Finally, Digital Image Correlation (DIC) should be considered as a potential method to reduce uncertainties in strain measurements, particularly to avoid tricky and debated corrections related to tensile set-up compliance and fibre slipping and seating in the grips [67].

Finally, this round-robin study provides a unique database and associated analysis for better identifying and reducing sources of epistemic uncertainty, as well as for enhancing experimental procedures and post-processing methods associated with the characterisation of single individual fibres. It represents an additional step towards overcoming the challenge of accurately quantifying the stochastic uncertainty arising from the inherent randomness of synthetic and natural fibres. This study also benefits from providing and making accessible to the scientific community a vast database that can be further used for a variety of statistical analyses.

Acknowledgements

This work has been supported by the CNRS research network (GDR 2024) Multiscale mechanics of fibrous media and by EIPHI Graduate School under ("ANR-17-EURE-0002"). The authors thank also the CNRS for the funding of the CARAFIB project (PEPS 2023). NLM and SC (Laboratory A, C2MA) thank Cyrielle Blanc for her contribution to the experimental measurements. PJJD and FM (Laboratory F, LaMCoS) would like to thank Théo Abdul-Ghafour and Achille Omgba Betené for their contribution to the experimental measurements. VP (Laboratory C, FEMTO-ST) thanks Professor Stefano Amaducci from Università Cattolica del Sacro Cuore, Piacenza, Italy for providing the hemp fibres. We also thank an anonymous referee for particularly helpful comments and for suggesting very valuable improvements on an earlier version of this manuscript.

References

[1] Bourmaud A, Beaugrand J, Shah DU, Placet V, Baley C. Towards the design of high-performance plant fibre composites. Prog Mater Sci 2018;97:347–408. https://doi.org/10.1016/j.pmatsci.2018.05.005.

[2] Baley C, Gomina M, Breard J, Bourmaud A, Davies P. Variability of mechanical properties of flax fibres for composite reinforcement. A review. Ind Crops Prod 2020;145.

https://doi.org/10.1016/j.indcrop.2019.111984.

[3] Richely E, Bourmaud A, Placet V, Guessasma S, Beaugrand J. A critical review of the ultrastructure, mechanics and modelling of flax fibres and their defects. Prog Mater Sci 2022;124:100851. https://doi.org/10.1016/j.pmatsci.2021.100851.

[4] Summerscales J, Virk AS, Hall W. Fibre area correction factors (FACF) for the extended rules-of-mixtures for natural fibre reinforced composites. Mater Today Proc 2020;31:S318–20. https://doi.org/https://doi.org/10.1016/j.matpr.2020.01.552.

[5] Ribeiro MM, Pinheiro MA, Rodrigues J da S, Ramos RPB, Corrêa A de C, Monteiro SN, et al. Comparison of Young’s Modulus of Continuous and Aligned Lignocellulosic Jute and Mallow Fibers Reinforced Polyester Composites Determined Both Experimentally and from Theoretical Prediction Models. Polymers (Basel) 2022;14. https://doi.org/10.3390/polym14030401.

[6] Bensadoun F, Verpoest I, Baets J, Müssig J, Graupner N, Davies P, et al. Impregnated fibre bundle test for natural fibres used in composites. J Reinf Plast Compos 2017;36:942–57. https://doi.org/10.1177/0731684417695461.

[7] Shah DU, Nag RK, Clifford MJ. Why do we observe significant differences between measured and 'back-calculated' properties of natural fibres? Cellulose 2016;23:1481–90. https://doi.org/10.1007/s10570-016-0926-x.

[8] Parameswaranpillai J, Gopi JA, Radoor S, D. MDC, Krishnasamy S, Deshmukh K, et al. Turning waste plant fibers into advanced plant fiber reinforced polymer composites: A comprehensive review. Compos Part C Open Access 2023;10:100333. https://doi.org/https://doi.org/10.1016/j.jcomc.2022.100333.

[9] Viotti C, Albrecht K, Amaducci S, Bardos P, Bertheau C, Blaudez D, et al. Nettle, a Long-Known Fiber Plant with New Perspectives. Materials (Basel) 2022;15. https://doi.org/10.3390/ma15124288.

[10] Sarasini F, Fiore V. A systematic literature review on less common natural fibres and their biocomposites. J Clean Prod 2018;195:240–67. https://doi.org/https://doi.org/10.1016/j.jclepro.2018.05.197.

[11] Ndoumou RL, Soulat D, Labanieh AR, Ferreira M, Meva'a L, Atangana Ateba J. Characterization of Tensile Properties of Cola lepidota Fibers. Fibers 2022;10. https://doi.org/10.3390/fib10010006.

[12] Castellano J, Marrero MD, Ortega Z, Romero F, Benitez AN, Ventura MR. Opuntia spp. Fibre Characterisation to Obtain Sustainable Materials in the Composites Field. Polymers (Basel) 2021;13. https://doi.org/10.3390/polym13132085.

[13] Zimniewska M. Hemp Fibre Properties and Processing Target Textile: A Review. Materials (Basel) 2022;15. https://doi.org/10.3390/ma15051901.

[14] Hassan T, Jamshaid H, Mishra R, Khan MQ, Petru M, Novak J, et al. Acoustic, Mechanical and Thermal Properties of Green Composites Reinforced with Natural Fibers Waste. Polymers (Basel) 2020;12. https://doi.org/10.3390/polym12030654.

[15] Yu X, Fan W, Azwar E, Ge S, Xia C, Sun Y, et al. Twisting in improving processing of waste-derived yarn into high-performance reinforced composite. J Clean Prod 2021;317:128446. https://doi.org/https://doi.org/10.1016/j.jclepro.2021.128446.

[16] Ivars J, Labanieh AR, Soulat D. Effect of the Fibre Orientation Distribution on the Mechanical and Preforming Behaviour of Nonwoven Preform Made of Recycled Carbon Fibres. Fibers 2021;9. https://doi.org/10.3390/fib9120082.

[17] Barnett PR, Ghossein HK. A Review of Recent Developments in Composites Made of Recycled Carbon Fiber Textiles. Textiles 2021;1:433–65. https://doi.org/10.3390/textiles1030023.

[18] Xue Y, Du Y, Elder S, Wang K, Zhang J. Temperature and loading rate effects on tensile properties of kenaf bast fiber bundles and composites. Compos Part B Eng 2009;40:189–96. https://doi.org/10.1016/j.compositesb.2008.11.009.

[19] Khurshid MF, Hengstermann M, Hasan MMB, Abdkader A, Cherif C. Recent developments in the processing of waste carbon fibre for thermoplastic composites – A review. J Compos Mater 2020;54:1925–44. https://doi.org/10.1177/0021998319886043.

[20] Pimenta S, Pinho ST. The effect of recycling on the mechanical response of carbon fibres and their composites. Compos Struct 2012;94:3669–84. https://doi.org/https://doi.org/10.1016/j.compstruct.2012.05.024.

[21] van de Werken N, Reese MS, Taha MR, Tehrani M. Investigating the effects of fiber surface treatment and alignment on mechanical properties of recycled carbon fiber composites. Compos Part A Appl Sci Manuf 2019;119:38–47. https://doi.org/10.1016/j.compositesa.2019.01.012.

[22] Mesquita F, Bucknell S, Leray Y, Lomov S V, Swolfs Y. Single carbon and glass fibre properties characterised using large data sets obtained through automated single fibre tensile testing. Compos Part A Appl Sci Manuf 2021;145:106389. https://doi.org/https://doi.org/10.1016/j.compositesa.2021.106389.

[23] Meek N, Penumadu D. Nonlinear elastic response of pan based carbon fiber to tensile loading and relations to microstructure. Carbon N Y 2021;178:133–43. https://doi.org/10.1016/j.carbon.2021.03.012.

[24] De Prez J, Van Vuure AW, Ivens J, Aerts G, Van de Voorde I. Effect of enzymatic treatment of flax on fineness of fibers and mechanical performance of composites. Compos Part A Appl Sci Manuf 2019;123:190–9. https://doi.org/10.1016/j.compositesa.2019.05.007.

[25] ASTM C1557 Standard test method for tensile strength and Young's modulus of fibers 2008.

[26] ASTM D3822-07 Standard test method for tensile properties of single textile fibers, ASTM; 2007.

[27] AFNOR. NF T25-501-2. Fibres de renfort - Fibres de lin pour composites plastiques - Partie 2 : détermination des propriétés en traction des fibres élémentaires. 2015.

[28] Charlet K, Baley C, Morvan C, Jernot JP, Gomina M, Bréard J. Characteristics of Hermès flax fibres as a function of their location in the stem and properties of the derived unidirectional composites. Compos Part A Appl Sci Manuf 2007;38:1912–21. https://doi.org/10.1016/j.compositesa.2007.03.006.

[29] Amarasinghe P, Pierre C, Moussavi M, Geremew A, Woldesenbet S, Weerasooriya A. The morphological and anatomical variability of the stems of an industrial hemp collection and the properties of its fibres. Heliyon 2022;8:e09276. https://doi.org/10.1016/j.heliyon.2022.e09276.

[30] Haag K, Müssig J. Scatter in tensile properties of flax fibre bundles: influence of determination and calculation of the cross-sectional area. J Mater Sci 2016;51:7907–17. https://doi.org/10.1007/s10853-016-0052-z.

[31] Lefeuvre A, Bourmaud A, Morvan C, Baley C. Tensile properties of elementary fibres of flax and glass: Analysis of reproducibility and scattering. Mater Lett 2014;130. https://doi.org/10.1016/j.matlet.2014.05.115.

[32] Islam F, Joannès S, Laiarinandrasana L. Evaluation of Critical Parameters in Tensile Strength Measurement of Single Fibres. J Compos Sci 2019;3. https://doi.org/10.3390/jcs3030069.

[33] Joannès S, Islam F, Laiarinandrasana L. Uncertainty in Fibre Strength Characterisation Due to Uncertainty in Measurement and Sampling Randomness. Appl Compos Mater 2020;27:165–84. https://doi.org/10.1007/s10443-020-09803-9.

[34] Lefeuvre A, Bourmaud A, Lebrun L, Morvan C, Baley C. A study of the yearly reproducibility of flax fiber tensile properties. Ind Crops Prod 2013;50. https://doi.org/10.1016/j.indcrop.2013.07.035.

[35] Charlet K, Jernot JP, Eve S, Gomina M, Bréard J. Multi-scale morphological characterisation of flax: From the stem to the fibrils. Carbohydr Polym 2010;82:54–61. https://doi.org/10.1016/j.carbpol.2010.04.022.

[36] Garat W, Corn S, Le Moigne N, Beaugrand J, Bergeret A. Analysis of the morphometric variations in natural fibres by automated laser scanning: Towards an efficient and reliable assessment of the cross-sectional area. Compos Part A Appl Sci Manuf 2018;108:114–23. https://doi.org/10.1016/j.compositesa.2018.02.018.

[37] Islam F, Joannès S, Bucknell S, Leray Y, Bunsell A, Laiarinandrasana L. Investigation of tensile strength and dimensional variation of T700 carbon fibres using an improved experimental setup. J Reinf Plast Compos 2020;39:144–62. https://doi.org/10.1177/0731684419873712.

[38] Charlet K, Jernot J-P, Breard J, Gomina M. Scattering of morphological and mechanical properties of flax fibres. Ind Crops Prod 2010;32:220–4. https://doi.org/10.1016/j.indcrop.2010.04.015.

[39] Grégoire M, De Luycker E, Ouagne P. Elementary Liber Fibres Characterisation: Bias from the Noncylindricity and Morphological Evolution along the Fibre. Fibers 2023;11:45. https://doi.org/10.3390/fib11050045.

[40] Baley C. Analysis of the flax fibres tensile behaviour and analysis of the tensile stiffness increase. Compos Part A Appl Sci Manuf 2002;33:939–48. https://doi.org/10.1016/S1359-835X(02)00040-4.

[41] Duval A, Bourmaud A, Augier L, Baley C. Influence of the sampling area of the stem on the mechanical properties of hemp fibers. Mater Lett 2011;65:797–800. https://doi.org/10.1016/j.matlet.2010.11.053.

[42] Placet V, Cissé O, Lamine Boubakar M. Nonlinear tensile behaviour of elementary hemp fibres. Part I: Investigation of the possible origins using repeated progressive loading with in situ microscopic observations. Compos Part A Appl Sci Manuf 2014;56:319–27. https://doi.org/10.1016/j.compositesa.2012.11.019.

[43] Lefeuvre A, Bourmaud A, Morvan C, Baley C. Elementary flax fibre tensile properties: Correlation between stress–strain behaviour and fibre composition. Ind Crops Prod 2014;52:762–9. https://doi.org/10.1016/j.indcrop.2013.11.043.

[44] Trivaudey F, Placet V, Guicheret-Retel V, Boubakar ML. Nonlinear tensile behaviour of elementary hemp fibres. Part II: Modelling using an anisotropic viscoelastic constitutive law in a material rotating frame. Compos Part A Appl Sci Manuf 2015;68:346–55. https://doi.org/10.1016/j.compositesa.2014.10.020.

[45] Del Masto A, Trivaudey F, Guicheret-Retel V, Placet V, Boubakar L. Nonlinear tensile behaviour of elementary hemp fibres: a numerical investigation of the relationships between 3D geometry and tensile behaviour. J Mater Sci 2017;52:6591–610. https://doi.org/10.1007/s10853-017-0896-x.

[46] Del Masto A, Trivaudey F, Guicheret-Retel V, Placet V, Boubakar L. Investigation of the possible origins of the differences in mechanical properties of hemp and flax fibres: A numerical study based on sensitivity analysis. Compos Part A Appl Sci Manuf 2019;124:105488. https://doi.org/10.1016/j.compositesa.2019.105488.

[47] Nuez L, Richely E, Perez J, Guessasma S, Beaugrand J, D'Arras P, et al. Exploring the effect of relative

humidity on dynamic evolution of flax fibre's microfibril angle through in situ tensile tests under synchrotron X-ray diffraction. Ind Crops Prod 2022;188:115592. https://doi.org/10.1016/j.indcrop.2022.115592.

[48] Richely E, Nuez L, Pérez J, Rivard C, Baley C, Bourmaud A, et al. Influence of defects on the tensile behaviour of flax fibres: Cellulose microfibrils evolution by synchrotron X-ray diffraction and finite element modelling. Compos Part C Open Access 2022;9:100300. https://doi.org/10.1016/j.jcomc.2022.100300.

[49] Engelbrecht-Wiggans AE, Forster AL. Analysis of strain correction procedures for single fiber tensile testing. Compos Part A Appl Sci Manuf 2023;167:107411. https://doi.org/10.1016/j.compositesa.2022.107411.

[50] Thomason JL, Carruthers J, Kelly J, Johnson G. Fibre cross-section determination and variability in sisal and flax and its effects on fibre performance characterisation. Compos Sci Technol 2011;71:1008–15. https://doi.org/10.1016/j.compscitech.2011.03.007.

[51] Huguet E, Corn S, Moigne N Le, Ienny P. Mechanical behavior of flax fiber bundles during cyclic tensile tests in a controlled humid. ICCM 23 - 23rd Int. Conf. Compos. Mater., Belfast: 2023.

[52] Kiureghian A Der, Ditlevsen O. Aleatory or epistemic? Does it matter? Struct Saf 2009;31:105–12. https://doi.org/10.1016/j.strusafe.2008.06.020.

[53] Cline J, Wu V, Moy P. Assessment of the Tensile properties for single fibers. Technical report ARL-TR-8299. Aberdeen Proving Ground, MD 21005, USA: 2018.

[54] Richard C, Bresson B, Bès M, Schittecatte L, Le Roux S, Didane N, et al. Mechanisms of damage and fracture of aramid fibers: Focus on the role of microfibril cooperativity in fracture toughness. J Polym Sci 2023;61:2549–58. https://doi.org/10.1002/pol.20230400.

[55] Kotera M, Nakai A, Saito M, Izu T, Nishino T. Elastic Modulus of the Crystalline Regions of Poly (p-phenylene terephthalamide) Single Fiber Using SPring-8 Synchrotron Radiation. Polym J 2007;39:1295–9. https://doi.org/10.1295/polymj.PJ2007074.

[56] Bourmaud A, Beaugrand J, Shah DU, Placet V, Baley C. Towards the design of high-performance plant fibre composites. Prog Mater Sci 2018;97:347–408. https://doi.org/10.1016/j.pmatsci.2018.05.005.

[57] Sala B, Surkova P, Sanctorum M, Guicheret-Retel V, Trivaudey F, Boubakar L, et al. Variability in the elastic and time-delayed properties of structural hemp fibre composites. Compos Part A Appl Sci Manuf 2022;161:107116. https://doi.org/10.1016/j.compositesa.2022.107116.

[58] Gabrion X, Koolen G, Grégoire M, Musio S, Bar M, Botturi D, et al. Influence of industrial processing parameters on the effective properties of long aligned European hemp fibres in composite materials. Compos Part A Appl Sci Manuf 2022;157:106915.

[59] Garat W, Le Moigne N, Corn S, Beaugrand J, Bergeret A. Swelling of natural fibre bundles under hygro- and hydrothermal conditions: Determination of hydric expansion coefficients by automated laser scanning. Compos Part A Appl Sci Manuf 2020;131. https://doi.org/10.1016/j.compositesa.2020.105803.

[60] Garat W, Corn S, Le Moigne N, Beaugrand J, Ienny P, Bergeret A. Dimensional Variations and Mechanical Behavior of Various Plant Fibre Species under Controlled Hydro / Hygrothermal Conditions. Rev Des Compos Des Matériaux Avancés 2019;29:299–304. https://doi.org/10.18280/rcma.290504.

[61] Garat W, Le Moigne N, Corn S, Beaugrand J, Bergeret A. Swelling of natural fibre bundles under hygro- and hydrothermal conditions: Determination of hydric expansion coefficients by automated laser scanning. Compos Part A Appl Sci Manuf 2020;131:105803.

https://doi.org/10.1016/j.compositesa.2020.105803.

[62] Le Duigou A, Merotte J, Bourmaud A, Davies P, Belhouli K, Baley C. Hygroscopic expansion: A key point to describe natural fibre/polymer matrix interface bond strength. Compos Sci Technol 2017;151:228–33. https://doi.org/10.1016/j.compscitech.2017.08.028.

[63] Islam F. Probabilistic single fibre characterisation to improve stochastic strength modelling of unidirectional composites. Université Paris sciences et lettres, 2020.

[64] Mesquita F, Bucknell S, Leray Y, Lomov S V., Swolfs Y. Single carbon and glass fibre properties characterised using large data sets obtained through automated single fibre tensile testing. Compos Part A Appl Sci Manuf 2021;145:106389. https://doi.org/10.1016/j.compositesa.2021.106389.

[65] Huguet E, Corn S, Le Moigne N, Ienny P. Contribution à la caractérisation du comportement mécanique de fibres végétales en environnement contrôlé: fiabilisation d'un banc test de mesure en traction. JJC ECOCOMP 2022 -5e édition des Journées Jeunes Cherch. en Eco-composites Compos. Bio-sourcés, Groix: 2022.

[66] del Masto A. Transition d'échelle entre fibre végétale et composite UD : propagation de la variabilité et des non-linéarités. Université Bourgogne Franche-Comté, 2018.

[67] Huguet E, Corn S, Le Moigne N, Ienny P. Single-fibre tensile testing of plant fibres: set-up compliance as a key parameter for reliable assessment of their mechanical behaviour. Ind Crops Prod 2024 (under review).

Declaration of interests

☒ The authors declare that they have no known competing financial interests or personal relationships that could have appeared to influence the work reported in this paper.

☒ The authors declare the following financial interests/personal relationships which may be considered as potential competing interests:

Thomas Jeannin Gilles Arnold

Alain Bourmaud Stéphane Corn

Emmanuel De Luycker 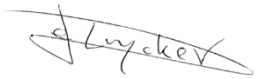

Pierre J.J. Dumont 

Manuela Ferreira 

Camille François 

Marie Grégoire 

Omar Harzallah 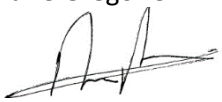

Julie Heurtel 

Sébastien Joannès 

Antoine Kervoelen 

Ahmad Rashed Labanieh 

Nicolas Le Moigne 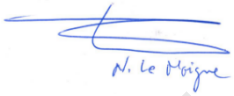

Florian Martoïa 

Laurent Orgéas 

Pierre Ouagne 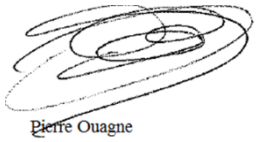

Damien Soulat 

Alexandre Vivet 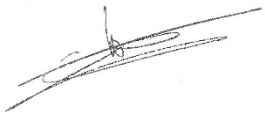

Vincent Placet